Kinetic model for plasma-based ion implantation of a short, cylindrical tube with auxiliary electrode

T. E. Sheridan[a)]
Space Plasma and Plasma Processing Group, Plasma Research Laboratory, Research School of Physical Sciences and Engineering, Australian National University, Canberra, Australian Capital Territory 0200, Australia

T. K. Kwok and P. K. Chu
Department of Physics and Material Science, City University of Hong Kong, Kowloon, Hong Kong

(Received 23 November 1997; accepted for publication 5 February 1998)

Plasma-based ion implantation of the inner surface of a short, cylindrical tube is modeled using a two-dimensional particle-in-cell simulation. An auxiliary electrode, here a coaxial anode, is used to increase the ion impact energy. Initially, ions inside the tube impact the inner surface at approximately normal angles. At later times, ions enter the tube from the exterior plasma and impact predominantly near its center at glancing angles. Ions are found to cross the midplane of the tube and in some cases to pass completely through the tube, in contrast to the predictions of the "collisionless" fluid model. The total incident dose is greatest around the center of the tube, and least at its ends. © *1998 American Institute of Physics.* [S0003-6951(98)00615-9]

A continuing impediment to the profitable application of plasma-based ion implantation (PBII) for inner surface modification is that of low ion impact energy. Briefly, the problem is this. If the inner radius r_{in} of a cylindrical bore or tube is less than the ion-matrix overlap length[1]

$$s_1 = \sqrt{\frac{-4\epsilon_0 \phi_{max}}{e n_0}}, \tag{1}$$

where n_0 is the plasma density and ϕ_{max} is the maximum negative target bias, then the ion space charge in the bore is insufficient to fully shield out the applied potential. Consequently, the potential drop from the axis to the inner wall is less than ϕ_{max}, and the ion impact energy is correspondingly reduced. This problem is exacerbated as ions are lost to the target since there is then even less space charge to support the potential drop.[2] For example, for $r_{in}=s_1$, the average ion impact energy is 25% of $|e\phi_{max}|$ (for singly ionized ions), while the maximum impact energy is but[2,3] 36.8% of $|e\phi_{max}|$. (For $r_{in}>s_1$, the ion impact energy increases[4] with r_{in} and asymptotically approaches $|e\phi_{max}|$.)

Recently, it has been suggested[5,6] that the use of an auxiliary electrode, in this case a grounded coaxial anode, can raise the average ion impact energy at the inner surface. This is because the auxiliary electrode ensures that the potential drop always equals the applied potential, thereby preventing the decay of the radial electric field. (In general, auxiliary electrodes could be used in other geometries to either increase the ion impact energy or to sculpt the flux.) The one-dimensional case has been considered in some detail.[7,8] However, one-dimensional theory is only valid when the length of the tube is large compared to its radius, and then only far from its ends.

A two-dimensional, "collisionless" fluid simulation[9] for PBII of a short, cylindrical tube with an auxiliary electrode has been reported. However, for a trench geometry (the planar analog of a hole), a comparison between fluid[10] and kinetic[11] simulations indicates that the "collisionless" fluid model does not provide a full description of the ion dynamics. In the kinetic simulation[11] (a particle-in-cell simulation), it was found that ion trajectories crossed. This crossing cannot be resolved by the fluid model, which requires that the ion velocity is single-valued everywhere. Consequently, a "collisionless" fluid simulation of inner surface implantation may not completely describe sheath expansion and the associated ion trajectories.

In this letter, we consider plasma-based ion implantation of a short, cylindrical tube with an auxiliary electrode. Our results are new, in that this is the first investigation in the context of PBII of an "open" geometry (i.e., a target that is open to the plasma at both ends) using a kinetic simulation. This geometry demonstrates new aspects of ion dynamics during sheath expansion that are particularly relevant to the PBII process—aspects not captured by the fluid model. In particular, ions are free to flow through the tube so that ions entering one end may be implanted at the other, or even pass through the tube and re-enter the sheath.

The target geometry is that of a short cylindrical tube (e.g., a bushing or ring), as shown in Fig. 1. The inner radius of the tube is r_{in}, the outer is r_{out}, and its full length is $2L$. Cylindrical symmetry is assumed. To improve the ion impact energy on the inner surface, we use a grounded, coaxial, auxiliary electrode of radius r_{aux}. The midplane of the tube ($z=0$) is a symmetry plane—the axial electric field $E_z=0$ there, while ions that cross the midplane from $z>0$ are reflected in z, thereby representing ions coming from $z<0$.

We adopt the standard model of the PBII plasma. Initially, we assume that the plasma is uniform everywhere, so that the ion density n_i and electron density n_e both equal n_0, the ion velocities $\mathbf{v}_i=0$ and the potential $\phi=0$. The ions are cold and ion motion is collisionless. The electron density is given by the Boltzmann relation

[a)]Electronic mail: terry.sheridan@anu.edu.au

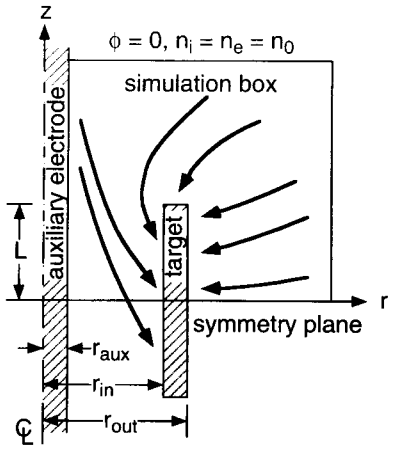

FIG. 1. Schematic of the implantation geometry. The solution domain is cylindrically symmetric so that the target is a short cylindrical tube. Possible ion trajectories are indicated.

$$n_e = n_0 \exp(\phi/T_e), \tag{2}$$

where T_e is the electron temperature in eV. At time $t=0$, the target potential ϕ_t is ramped from zero to a final negative bias $\phi_{\max}$ with a rise time t_r. That is, the target bias is given by

$$\phi_t = \phi_{\max}[1-\exp(-t/t_r)]. \tag{3}$$

The plasma responds self-consistently to the change in target potential—electrons are expelled from the vicinity of the target, while ions are drawn toward it, causing the sheath to expand. Ions are modeled using the method of particles. That is, we solve the ion-Vlasov equation by representing the ion distribution function at each point with a finite number of ion simulation particles. In contrast, a fluid model *approximates* the ion distribution function at each point using only a few moments, e.g., the density and average velocity.

Model variables are nondimensionalized in the normal way: distance by s_1, time by the inverse ion plasma frequency ω_{pi}^{-1}, and potential by the maximum target potential $\phi_{\max}$. After nondimensionalization, the model contains geometrical parameters describing the target and temporal parameters describing the voltage pulse. In addition, Poisson's equation contains the parameter $\phi_{\max}/T_e$. Fortunately, to model sheath dynamics during PBII, it is not necessary that we use a realistic value for this ratio (typically 10^4), but merely a value $\gg 1$.

We have modeled the following physical problem: $r_{aux}=0.1s_1$, $r_{in}=1s_1$, $r_{out}=1.1s_1$, $L=0.5s_1$ (i.e., the full length of the tube is s_1) and $t_r\omega_{pi}=1/16$. Here $t_r \ll \omega_{pi}^{-1}$, which is effectively the zero-rise time case. These parameters are essentially those used for the fluid simulation in Ref. 9. Typical PBII parameters are $\phi_{\max}=-40$ kV and $n_0=10^9$ cm^{-3} of N_2^+, so $s_1=9.4$ cm and $t_r=7.9$ ns. PIC simulation parameters were: grid spacing=1 Debye length, time step=$1/256\omega_{pi}^{-1}$ and $\phi_{\max}=625\,T_e$, so $s_1=50$ D lengths. The model was solved on a 150×125 grid ($3s_1\times2.5s_1$), and 100 ion particles were initially placed in each cell (1.8 million initial particles) using the "uniform-random" method.[12] The simulation was stopped at $t\omega_{pi}=40$, by which time the sheath has nearly reached the boundaries.

The temporal evolution of the ion density is shown in Fig. 2 for $t\omega_{pi}=5$, 10, 15, and 40. Here $t\omega_{pi}=5$ [Fig. 2(a)] is

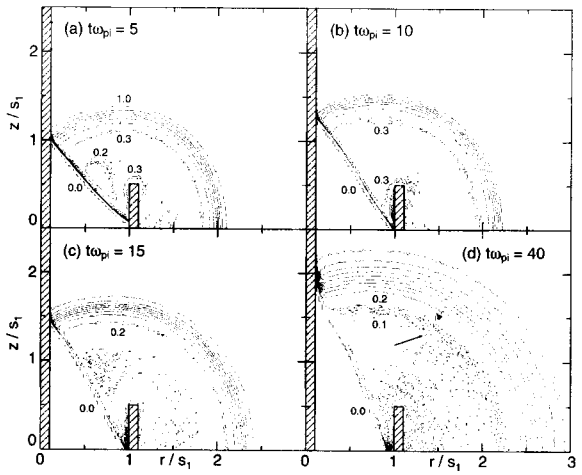

FIG. 2. Ion density contours for (a) $t\omega_{pi}=5$, (b) $t\omega_{pi}=10$, (c) $t\omega_{pi}=15$, and (d) $t\omega_{pi}=40$. Contours are labeled by the normalized ion density n_i/n_0, where $n_i/n_0=1$ in the ambient plasma. The arrow in (d) indicates ions that have passed through the tube and re-entered the sheath.

just after the end of the "ion-matrix phase," during which time ions inside the ion-matrix sheath are accelerated to the target. Since $r_{in}=s_1$, all ions between the auxiliary electrode and inner surface are caught in the ion-matrix sheath. For the parameters used here, the ion-matrix phase lasts until $t\omega_{pi}\approx3.6$. At this time, the ion density on the symmetry plane ($z=0$) falls to zero. Ions are then seen to be focused on the top of the tube, as well as along a diagonal line stretching from the auxiliary electrode to the inner surface (i.e., a conical surface), which we henceforth refer to as the "inner beam." Here the sheath and target sizes are comparable, so that one-dimensional theory[7,8] cannot be expected to quantitatively describe sheath expansion either inside or outside the tube.

After the ion-matrix phase has ended, the second stage of sheath expansion begins as ions initially outside the tube enter it, as shown in Fig. 2(b) for $t\omega_{pi}=10$. At this time, the inner beam has just breached the symmetry plane—the ion density at $z=0$ has risen above zero. This behavior is not seen for the fluid model,[9] and is in fact, not allowed by it. Due to symmetry at $z=0$, the ion flux there must equal zero. The only way this condition can be satisfied in the fluid model is by requiring the z component of the fluid velocity there equal to zero. However, in the kinetic model this condition can also be satisfied by equal fluxes of ions flowing upward and downward. In addition to the inner beam, a second region of enhanced ion density can be seen on the inner surface at $z/s_1\approx0.2$. This focusing is due to ions that start with $r\gtrsim r_{in}$ and are attracted to the the top of the tube, but miss and enter, as indicated in Fig. 1. We refer to this stream as the "outer beam." (In the fluid simulation,[9] these trajectories cause the radial component of the fluid velocity to become negative inside the bore.)

By $t\omega_{pi}=15$ [Fig. 2(c)], the inner beam has clearly crossed the symmetry plane, and is now incident on the upper half of the target ($z>0$) from below ($z<0$), while the outer beam is still incident from above (as will be demonstrated below). At these later times, the potential structure in the sheath changes quite slowly, (i.e., sheath expansion is

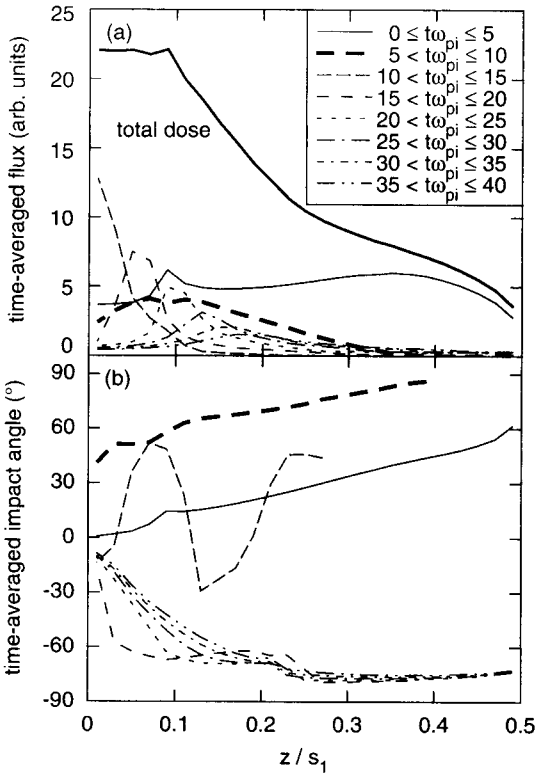

FIG. 3. Time-averaged (a) ion flux and (b) average impact angle. Angles greater than zero indicate ion impact from above, while those less than zero indicate impact from below (i.e., after having passed through the symmetry plane).

quasi-static), so that the locations on the inner surface on which ions are focused also change slowly.

At $t\omega_{pi}=40$ [Fig. 2(d)], both the inner and outer beams have crossed the symmetry plane and are incident from below. Interestingly, a beam of ions (indicated by the arrow) can be seen at the sheath edge after having passed completely through the tube. Again, such a phenomenon cannot be resolved using fluid ions, as it requires that the ion velocity is multi-valued.

The time-averaged ion flux and average impact angle on the inner surface are shown in Fig. 3. Positive angles represent ions that impact the target with negative v_z (i.e., from above), while negative angles represent ions with positive v_z. (The average impact angle is defined only where the flux is nonzero.) For $t\omega_{pi}\leq 5$, the flux near the middle of the tube is depressed since all the nearby ions have impacted by $t\omega_{pi}\leq 3.6$, while the impact angle is nearly zero around the center of the tube, sheath expansion here is somewhat one dimensional. There is also a large flux of ions to the top of the tube, with the flux least and the impact angle greatest at the corner. For $5<t\omega_{pi}\leq 10$, the impact angle is positive everywhere indicating that ions are predominantly incident from above, as shown in Fig. 2(b). For $10<t\omega_{pi}\leq 15$, some ions are incident from below, with the average impact angle near the symmetry plane becoming negative and the dose peaking there. That is, ions are passing through the symmetry plane. At later times, $t\omega_{pi}>15$, a peak in the dose can be seen moving up the inner surface toward the top of the tube while the average impact angle is uniformly negative, being $\approx -60°$ where the flux is largest. The total incident dose for the time simulated, $t\omega_{pi}\leq 40$, is strongly peaked near the center of the tube and falls significantly near the ends, with most of the dose there coming at early times. That is, the dose is depressed in the vicinity of the end of the tube in a manner analogous to that seen for a corner.[12]

In conclusion, sheath and ion dynamics during plasma-based ion implantation of a short, cylindrical tube have been investigated. An auxiliary electrode was used to increase the ion impact energy on the inner surface of the tube. Because the inner radius and the length of the tube were comparable to the sheath width, one-dimensional theory is inadequate. The ion flux to the inner surface consists essentially of two ion beams: an "inner" beam moving from smaller radii to larger, and an "outer" beam moving from larger radii to smaller. The kinetic model presented here predicts ion trajectories that are qualitatively different from those predicted by a "collisionless" fluid model.[9] Consequently, the fluid model should be used with care, and only in situations where the crossing of ion trajectories is nonexistent or negligible (e.g., one-dimensional problems); The trajectories of fluid elements and ions are not necessarily the same.

This work was supported by the Australian National University and by Hong Kong Research Grants Council Earmarked Grants Nos. 9040220 and 9040332 and City University of Hong Kong Strategic Grant No. 7000730.

[1] T. E. Sheridan, J. Appl. Phys. **74**, 4903 (1993).
[2] T. E. Sheridan, Phys. Plasmas **1**, 3485 (1994).
[3] T. E. Sheridan, Phys. Plasmas **4**, 3442 (1997).
[4] T. E. Sheridan, Phys. Plasmas **3**, 3507 (1996).
[5] Mu Sun, P. Zhu, and S. Z. Yang, J. Phys. D **29**, 274 (1996); T. E. Sheridan, *ibid.* **29**, 2733 (1996).
[6] X. C. Zeng, B. Y. Tang, and P. K. Chu, Appl. Phys. Lett. **69**, 3815 (1996).
[7] X. C. Zeng, T. K. Kwok, A. G. Liu, P. K. Chu, B. Y. Tang, and T. E. Sheridan, Appl. Phys. Lett. **71**, 1035 (1997).
[8] X. C. Zeng, T. K. Kwok, A. G. Liu, P. K. Chu, B. Y. Tang, and T. E. Sheridan, IEEE Trans. Plasma Sci. (in press).
[9] T. K. Kwok, T. E. Sheridan, X. C. Zeng, and P. K. Chu (unpublished).
[10] T. E. Sheridan, J. Phys. D **28**, 1094 (1995).
[11] T. E. Sheridan, IEEE Trans. Plasma Sci. **24**, 57 (1996).
[12] T. E. Sheridan, Appl. Phys. Lett. **68**, 1918 (1996).